Nonequilibrium phonon dynamics and electron distribution functions in InP and InAs

E. D. Grann and K. T. Tsen
Department of Physics and Astronomy, Arizona State University, Tempe, Arizona 85287

D. K. Ferry
Department of Electrical Engineering, Arizona State University, Tempe, Arizona 85287

(Received 11 September 1995; revised manuscript received 29 November 1995)

We have used subpicosecond laser pulses to study the generation of nonequilibrium LO phonons in both InP and InAs. These two semiconductors provide a contrast in that the decaying of the Raman signal probes different relaxation mechanisms. In InP, for example, we find that the decay of the Raman signal is dominated by the lifetime of the LO phonons. On the contrary, in InAs, our studies show that the decay of the Raman signal is governed by the time required for electrons to return to the Γ valley from the L valleys of the conduction bands. In addition, nonequilibrium electron distributions were also studied in InP and InAs. We have found that the single-particle-scattering spectrum in InAs can only be observed with the use of a much longer laser pulse width than subpicosecond as a result of electron intervalley scattering and very small electron effective mass.

I. INTRODUCTION

Excitation of semiconductors by ultrashort laser beams has been a major method of studying the dynamics of nonequilibrium electron and hole systems. The thermalization of the initial distributions of these carriers probes the details of the band structure and the dynamics of electron-phonon interactions. Since the original studies of picosecond Raman scattering in semiconductors,[1,2] it has become fairly well established that the cooling of the excited electron-hole plasma is dominated by the emission of optical phonons and that the deviation of the phonon population from equilibrium is quite important in determining the cooling time of the plasma.[3–9] Most of these studies have been carried out in the GaAs and/or $Al_{1-x}Ga_xAs$ system, and the dominant conclusion is that the cooling time of the hot electron-hole plasma is limited by the lifetime of the hot, nonequilibrium polar optical phonons in the system. Typically, this decay time is about 7 ps in bulk GaAs at $T=77$ K. A buildup of the nonequilibrium phonons creates a ''bottleneck'' in which the carriers and the phonon population reach a common energy and reabsorption of the phonons slows the overall cooling process of the carriers.

In this paper, we report time-resolved Raman measurements of nonequilibrium LO phonon populations in InP and InAs on the subpicosecond time scale and compare these experimental results with ensemble Monte Carlo calculations. The two semiconductors investigated here provide different qualitative behavior. The decay of the Raman signal in InP corresponds to a decay of the hot phonons, as in the case of GaAs, and the lifetime of this decay is determined primarily by the lifetime of the hot phonons. In the case of InAs, however, the decay is dominated by the long storage times of the carriers in the satellite valleys of InAs, in which the very low effective mass of the Γ valley causes a relatively slow return from the satellite valleys to the Γ valley. As a consequence, the cooling of the hot plasma, and the phonon population, is governed not by the phonon lifetime, but by the return time of the carriers from the satellite valleys. The nonequilibrium electron distributions were also studied in InP and InAs. Because of the long storage time of electrons in the satellite valleys of the latter material, a single-particle-scattering (SPS) spectrum can only be observed in InAs with the laser pulse of much longer than subpicosecond duration.

II. EXPERIMENTAL TECHNIQUE AND SAMPLES

The ultrashort laser pulses used in this experiment were generated from a DCM double-jet dye laser synchronously pumped by the second harmonic of a cw mode-locked yttrium aluminum garnet laser.[10] The pulses has an autocorrelation full width at half maximum of $\cong 800$ fs and an average power of $\cong 50$ mW, with a repetition rate of 76 MHz. In the time-resolved studies of nonequilibrium phonons, an appropriate analyzer was placed in front of the entrance slit of the double monochromator so that the scattered light from the pump pulse was effectively eliminated while the scattering from the probe pulse was allowed to be detected. The dye laser was chosen to operate at $\hbar\omega \cong 1.952$ eV. The anti-Stokes Raman signal was collected and analyzed by a standard Raman setup that included a charge-coupled device multichannel detection system.

For the studies of the electron distribution functions in InP, the same dye laser as described above was used except that the photon energy was $\hbar\omega \cong 1.91$ eV. For InAs, a cavity-dumped R6G dye laser that had a laser pulse width of $\cong 10$ ps and a photon energy of $\hbar\omega = 2.14$ eV was used for the observation of the SPS spectrum. The SPS spectra were taken in the $Z(X,Y)Z$ geometry, where $Z=(001)$, $X=(100)$, $Y=(010)$, so that only SPS associated with spin-density fluctuations was detected.[11,12] The SPS spectra were recorded with a Raman system equipped with a photon counting setup and a photomultiplier tube. Since the same laser pulses were used to both excite and probe the photoexcited carriers, the SPS results represent an average over the duration of the laser pulse width.

All of the experimental results reported here were taken at $T=300$ K. From the power density and the absorption coefficient of the pump pulses, the average photoexcited carrier density was estimated to be $\cong 3\times10^{15}$ cm^{-3} for the studies of nonequilibrium phonons and $\approx 10^{18}$ cm^{-3} for the studies of SPS spectra.

The undoped InP and InAs samples investigated in this work were grown by molecular-beam epitaxy on (001)-oriented InP and GaAs substrates, respectively. Both of the samples contain electron concentrations of $n\cong 5\times10^{14}$ cm^{-3}. The thickness of the epilayers was about 2 μm, which is sufficiently thick to relieve the lattice-mismatch-induced strain in the case of InAs.

III. MONTE CARLO SIMULATIONS

Simulations of the laser excited plasma were carried out by the ensemble Monte Carlo technique.[13] In this simulation, only the electrons were considered, as the population of the polar LO phonon modes was of primary interest. Hyperbolic energy bands were assumed for the various conduction bands, and all normal scattering processes were included. Interaction among the electrons was treated by a molecular-dynamics simulation technique, including the role of the exchange energy.[14,15]

On the short time scales, which depend upon the system being modeled, the electron distribution undergoes a significant perturbation in the typical time between scattering events. During the first picosecond of relaxation, a finite density of electrons will lose about 10% of their energy in each 0.1 ps through the emission of a phonon. During this initial decay, the plasma is modeled by an ensemble of electrons, and this approach has been successfully vectorized. Carrier-carrier scattering, however, is a multicarrier interaction that requires that these other carriers be available for the interaction. In general, a treatment similar to that for the phonons is possible only if the Coulomb interaction is treated as ''instantaneous,'' which is not likely to be the case. For this reason, we treat the Coulomb interaction via a real-space molecular-dynamics approach.[16]

Modeling of the nonequilibrium phonons was handled within the ensemble Monte Carlo procedure by a secondary self-scattering and rejection process pioneered by Lugli *et al.*[17] The buildup of the phonon population through emission and absorption processes was monitored throughout the simulation. The difference between the instantaneous value, for a given momentum wave vector, and some prescribed maximum value was used for the rejection technique. The presence of the nonequilibrium phonons slowed the energy relaxation of the hot carriers.

IV. EXPERIMENTAL RESULTS AND ANALYSIS

In Fig. 1, the time-resolved anti-Stokes Raman signal for an InP sample is shown as a function of the time delay between the pump and the probe pulses. The computed population of the polar LO phonons (with a wave vector appropriate to the range of wave vectors in the Raman scattering experiment) is also plotted. It is noted that the peak in phonon population is delayed relative to the zero time delay, and this corresponds to the need for the phonon cascade to occur

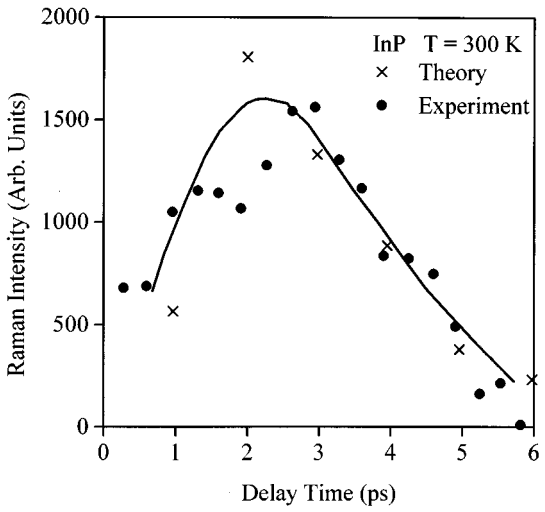

FIG. 1. Time-resolved anti-Stokes Raman signal as a function of the time delay for an InP sample at $T=300$ K. The solid circles are experimental data. The crosses are from ensemble Monte Carlo simulations. The solid curve is a guide to the eye for the theoretical fit to the data. The LO phonon lifetime deduced is 2.3 ps.

in order to build up the population. The typical photoexcited electron emits 10–12 LO phonons during the cascade and this leads to the observed delay in the Raman signal as this process requires about 2.5 ps. The lifetime of the nonequilibrium phonons in the Monte Carlo simulations has been taken to be 2.3 ps and this value leads to a good agreement between the experiment and the simulation. We note that this value of LO phonon population relaxation time is consistent with the results of von der Linde, Kuhl, and Rosengart in which the LO phonon lifetime in InP was measured to be $\cong 5$ ps at $T=77$ K.[18]

Figure 2 shows the time-resolved anti-Stokes Raman sig-

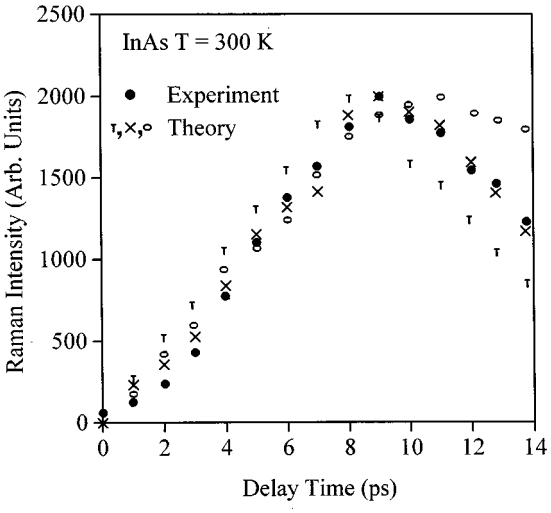

FIG. 2. Time-resolved anti-Stokes Raman signal as a function of the time delay for an InAs sample at $T=300$ K. The solid circles are experimental data. The theoretical calculations are from ensemble Monte Carlo simulations. The T's, crosses, and open circles correspond to the phonon lifetime and the coupling constant: 1.8 ps, 1.4×10^{8} eV/cm; 1.8 ps, 1.4×10^{9} eV/cm; 4 ps, 1.4×10^{9} eV/cm, respectively.

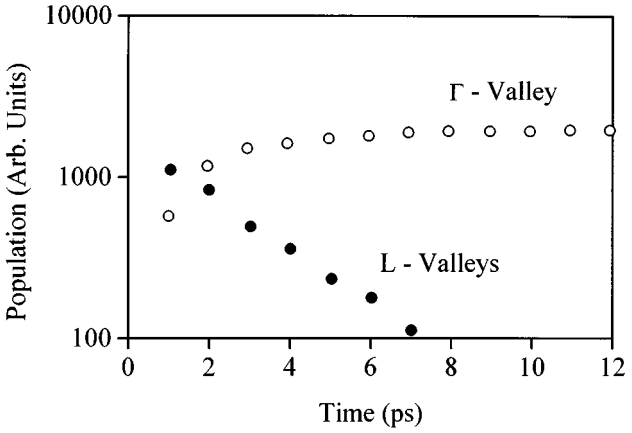

FIG. 3. The populations of the satellite L valleys (solid circles) and the Γ valley (open circles), as a function of time after initiation of the laser pulse. The laser pulse width is 0.6 ps.

nal and the computed LO phonon population from ensemble Monte Carlo simulations in an InAs sample. We have found that a phonon lifetime of about 1.8 ps had to be assumed in order to get a reasonable fit. In the case of InAs, a significant amount of carriers are scattered to the satellite valleys. Then, carriers returning from the satellite valleys emit more than 20 LO phonons in their cascade to the bottom of the conduction band. This together with the storage time in the satellite valleys lead to the long delay before the peak is observed in the Raman signal. In Fig. 3, we plot the electron population of the Γ and L valleys in InAs as predicted from ensemble Monte Carlo simulations. From this figure, it may be seen that the electron population of the L valleys decays with a time constant of approximately 6 ps. Apparently, the storage of the carriers in the L valleys leads to a continued generation of nonequilibrium phonons at long times, and the overall decay of the LO phonons replicates the decay of the electron population of the satellite valleys.

Figure 4(a) shows a SPS spectrum for an InP sample taken with a laser pulse width of $\cong 600$ fs, a photon energy of $\hbar\omega = 1.91$ eV, and carrier density $n \cong 10^{18}$ cm^{-3}. A theory originally developed by Hamilton and McWhorter[19] and properly modified by Chia, Sankey, and Tsen[20] to accommodate our current experimental conditions was employed to interpret the SPS spectrum. We have found that the data were best fit by the following parameter set: $T_e = 600$ K, $\tau = 15$ fs, and $\gamma = 13$ meV, where T_e is the effective electron temperature, τ is the electron collision time, and γ is the damping constant involved in the Raman scattering process. In other words, the electron distribution function is given by a Fermi-Dirac function with a temperature substantially higher than that of the lattice. We note that the deduced electron collision time is appropriate to that expected from electron-electron scattering at these densities.[14,15]

We did not observe any appreciable SPS signal when a laser pulse width of 600 fs was used in the InAs sample. This is consistent with our previous discussions on the nonequilibrium phonon dynamics in InAs, which demonstrated that the electrons were scattered very quickly (≈ 100 fs) from the Γ valley to the satellite valleys and returned to the Γ valley very slowly at a time constant of about 6 ps due to the very small effective mass in the Γ valley. Figure 4(b) shows a SPS

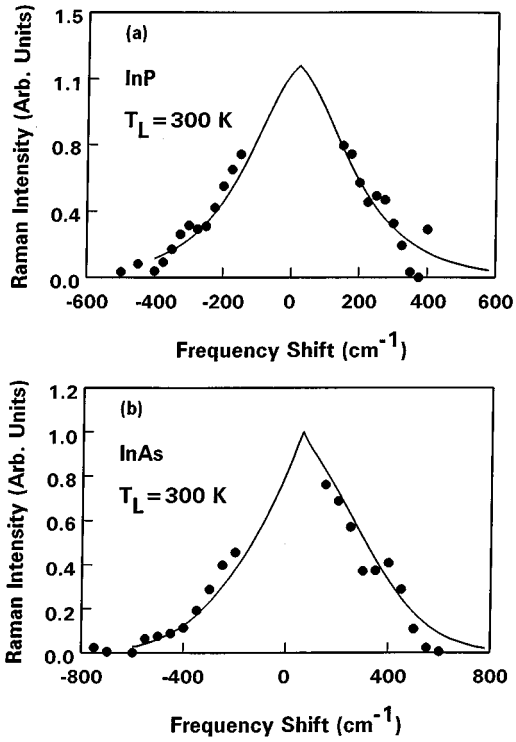

FIG. 4. Single-particle scattering spectrum for (a) InP and (b) InAs taken at $T = 300$ K. The photon energies and laser pulse widths are $\hbar\omega = 1.91$ eV, 0.6 ps for InP and 2.14 eV, 10 ps for InAs. The SPS spectra are very well described by a theory developed in Refs. 19 and 20.

spectrum for an InAs sample taken with a laser pulse width of $\cong 10$ ps, a photon energy of $\hbar\omega \cong 2.14$ eV, and an electron density of $n \cong 5 \times 10^{17}$ cm^{-3}. Again, we have used the theory by Chia, Sankey, and Tsen[20] to explain the SPS spectrum. The best fit parameter set is $T_e = 525$ K, $\tau = 40$ fs, $\gamma = 13$ meV.

We note that the temperature of the electron is quite high considering the fact that a laser pulse width of 10 ps was used in the experiment. However, we believe that this is reasonable because the cooling of the electrons in InAs has been greatly slowed by the effects of intervalley scattering together with the very small electron effective mass in the Γ valley.

V. DISCUSSION

In InP, with an excitation energy of $\hbar\omega = 1.952$ eV, carriers are excited from all three valence bands (the heavy-hole, light-hole, and split-off-hole bands). InP has a band gap of 1.28 eV at $T = 300$ K. The satellite valleys in InP lie considerably higher than those in the case of GaAs, and here it is assumed that the L valleys are 0.5 eV above the Γ-valley minimum, while the X valleys lie approximately 0.98 eV above the Γ-valley minimum.[23] Because of the high energy of the X valleys, there is no excitation into these valleys from the photoexcited electrons. On the other hand, a small number of electrons are scattered into the L valleys. However, by the time the peak of the phonon distribution occurs, essentially all of the carriers have returned to the Γ valley of the conduction band. The intervalley scattering process is quite

fast and a value of the Γ-L coupling constant of 7×10^8 eV/cm was used in our Monte Carlo simulations. This value is comparable to that of GaAs. Once the carriers are in the central valley of the conduction band, their cooling is dominated by a cascade of LO phonon emission processes. It is this cascade of emissions that leads to a buildup of the nonequilibrium phonon distribution. While a fraction of the carriers do transfer to the satellite L valleys, this number is so small that it essentially plays no role in the cooling of the hot plasma in InP. Rather, it is solely the phonon cascade and resultant nonequilibrium LO phonon distribution that governs the overall cooling of the hot plasma.

The model that we have used for InAs assumes that the L valleys are located approximately 0.72 eV above the Γ-valley minimum, while the X valleys are located approximately 0.98 eV above the Γ-valley minimum.[23] Since the band gap of InAs is so small (0.36 eV at $T=300$ K), the electrons are excited well up into the conduction band, and a significant fraction of these are scattered into the X valleys. The latter, however, are scattered into the L valleys quite rapidly, so that the main dynamics after the laser pulse is dominated by the Γ and L valleys. In contrast to the case of InP, however, the coupling between the Γ and L valleys is such that the low effective mass of InAs leads to a very slow return of the carriers from the L to Γ valleys. The anti-Stokes Raman signal in Fig. 2 for InAs depends primarily upon two factors—the phonon lifetime and the Γ-L coupling constant. We have found that the best fit parameter set to our experimental data is a phonon lifetime equal to 1.8 ps and a coupling constant equal to 1.4×10^9 eV/cm. To get a feeling of how these two factors influence the anti-Stokes Raman signal, we have also shown two theoretical calculations with a phonon lifetime of 1.8 ps and a coupling constant of 1.4×10^8 eV/cm; and a phonon lifetime of 4 ps and coupling constant of 1.4×10^9 eV/cm, respectively.

It is worth considering how the phonon lifetimes found here compare with those in other materials. In Fig. 5, we plot the LO phonon lifetime as a function of the bond length for various III-V semiconductors as indicated. The InP and InAs data are taken from the present measurements. The GaAs, GaP, and ZnSe data are from Refs. 21 and 22. To a good approximation, the LO phonon population relaxation time can be described by a d^{-10} dependence, where d is the bond length of the semiconductor. It is clear that the values found here fit this general trend, with the exception of ZnSe. While the data are not sufficiently to say whether this exponent should be 8 or 12 (e.g., we can say that it is 10 ± 0.5), it clearly is neither 5 nor 15. The phonon lifetime depends upon the third-order elastic constants. Weinreich[24] points out

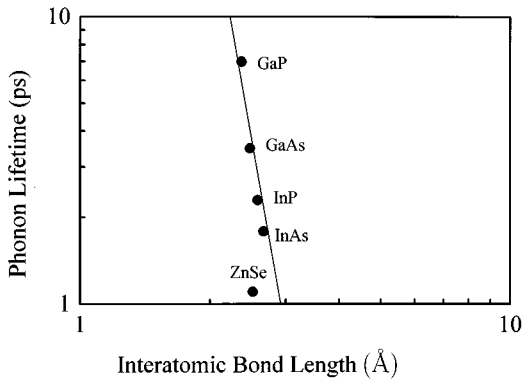

FIG. 5. The LO phonon population relaxation time as a function of the bond length for a variety of III-V semiconductors as indicated.

that the third-order elastic constant should have the same order of magnitude as the typical elastic modulus (stiffness constants), and Harrison[25] suggests that the latter should vary as d^{-5}. This would lead to a d^{-10} variation for the phonon lifetime, with adjustments coming from other parameters, of course. This is in keeping with the observed results of Fig. 5, and suggests that a wider range of materials should be investigated to confirm this behavior.

VI. CONCLUSION

We have used subpicosecond time-resolved Raman spectroscopy to investigate the nonequilibrium phonon dynamics in InP and InAs at $T=300$ K. We have found that these two semiconductors provide a contrast in that the decay of the Raman signal probes different relaxation mechanisms. In InP, we find that the decay of the Raman signal is dominated by the decay of the LO phonons. In contrast, in InAs, our studies demonstrate that the decay of the Raman signal is governed by the time required to return from the L valleys to the Γ valley of the conduction band. Because of this reason, single-particle scattering spectra in InAs can only be observed with a much longer laser pulse width ($\approx$10 ps).

ACKNOWLEDGMENTS

The authors would like to acknowledge helpful discussions with J. Kuhl of the Max-Planck Institute for Solid State Sciences. This work was supported by the National Science Foundation under Grant No. DMR-9301100 and by the Office of Naval Research.

[1] D. von der Linde, J. Kuhl, and H. Klingenburg, Phys. Rev. Lett. **44**, 1505 (1980).
[2] J. A. Kash, J. C. Tsang, and J. M. Hvam, Phys. Rev. Lett. **54**, 2151 (1985).
[3] W. Pötz and P. Kocevar, Phys. Rev. B **28**, 7040 (1980).
[4] J. Shah, A. Pinczuk, A. C. Gossard, and W. Wiegmann, Phys. Rev. Lett. **54**, 2045 (1985).
[5] P. Lugli and S. M. Goodnick, Phys. Rev. Lett. **59**, 716 (1987).
[6] S. Das Sarma, J. K. Jain, and R. Jalabert, Phys. Rev. B **37**, 1228 (1988).
[7] K. T. Tsen, R. P. Joshi, and D. K. Ferry, Phys. Rev. B **39**, 1446 (1989).
[8] R. P. Joshi and D. K. Ferry, Phys. Rev. B **39**, 1180 (1989).
[9] R. P. Joshi, K. T. Tsen, and D. K. Ferry, Phys. Rev. B **41**, 9899 (1990).
[10] K. T. Tsen and H. Morkoc, Phys. Rev. B **38**, 5615 (1988).

[11] M. V. Klein, in *Light Scattering in Solids I*, edited by M. Cardona and G. Guntherodt, Topics in Applied Physics Vol. 8 (Springer, New York, 1983), p. 151.
[12] G. Abstreiter, M. Cardona, and A. Pinczuk, in *Light Scattering in Solids III*, edited by M. Cardona and G. Guntherodt, Topics in Applied Physics Vol. 51 (Springer, New York, 1983), p. 5.
[13] D. K. Ferry, A. M. Kriman, M.-J. Kann, and R. P. Joshi, in *Monte Carlo Device Simulation: Full Band and Beyond*, edited by K. Hess (Kluwer, Norwall, MA, 1991), p. 99.
[14] M.-J. Kann, A. M. Kriman, and D. K. Ferry, Phys. Rev. B **41**, 12 659 (1990).
[15] A. M. Kriman, M.-J. Kann, D. K. Ferry, and R. P. Joshi, Phys. Rev. Lett. **65**, 1619 (1990).
[16] D. K. Ferry, A. M. Kriman, M.-J. Kann, and R. P. Joshi, Comput. Phys. Commun. **67**, 119 (1991).
[17] P. Lugli, C. Jacoboni, L. Reggiani, and P. Kocevar, Appl. Phys. Lett. **50**, 1251 (1987).
[18] D. von der Linde, J. Kuhl, and E. E. Rosengart, J. Phys. Soc. Jpn. Supp. A **49**, 653 (1980).
[19] D. C. Hamilton and A. L. McWhorter, in *Proceedings of the International Conference on Light Scattering Spectra of Solids*, edited by G. B. Wright (Springer, New York, 1969), p. 309.
[20] C. Chia, O. F. Sankey, and K. T. Tsen, Mod. Phys. Lett. B **7**, 331 (1993). Eq. (24).
[21] J. A. Kash, in *Light Scattering in Semiconductor Structures and Superlattices*, Vol. 273 of *NATO Advanced Studies Institute Series B: Physics*, edited by D. J. Lockwood and J. F. Young (Plenum Press, New York, 1991), p. 367.
[22] W. E. Bron, J. Kuhl, and B. K. Rhee, Phys. Rev. B **34**, 6961 (1986).
[23] D. K. Ferry, *Semiconductors* (Macmillan, New York, 1991).
[24] G. Weinreich, *Solids: Elementary Theory for Advanced Students* (Wiley, New York, 1965).
[25] W. A. Harrison, *Electronic Structure and the Properties of Solids* (Freeman, San Francisco, 1980).